DNS AND LES OF ESTIMATION AND CONTROL OF TRANSITION IN BOUNDARY LAYERS SUBJECT TO FREE-STREAM TURBULENCE

Luca Brandt,
Seyed M. Mojab, Antonios Monokrousos,
Philipp Schlatter and Dan S. Henningson
Linné Flow Centre, KTH Mechanics
Osquars Backe 18, SE-100 44 Stockholm, Sweden
antonios.monokrousos@mech.kth.se

INTRODUCTION

The aim of this study is to perform numerical simulations to apply feedback control to transitional boundary-layer flows. An efficient pseudo-spectral numerical code is used and modern control theories are incorporated into the controller design.

Control of wall-bounded transitional and turbulent flows is the object of the present investigation owing to the high potential benefits. Any reduction of the skin-friction, for example, implies relevant savings of the operational cost of commercial aircrafts and cargo ships. Numerical simulations and in particular direct numerical simulations (DNS) and large-eddy simulations (LES) have provided physical insight into the phenomena of transitional and turbulent flows, despite the fact that they are limited to simple and moderate Reynolds-number flows.

Recently, much effort is put in the combination of computational fluid dynamics and control theory (Bewley, 2001 and Kim, 2003). While early attempts of flow control were based on physical intuition or on a trial-and-error basis, more systematic approaches are now followed. Linear feedback control is considered in this project. Results from the application of linear optimal control theory confirm the importance of linear mechanisms in the nonlinear flows under consideration (Högberg and Henningson 2002). However, in the feedback perspective, full information on the flow is needed to compute the optimal control. This information is extracted from wall-measurements and the flow based on those the full flow field is estimated. The information problem is a limiting factor in the success of a control scheme, since, as a first step, it affects the whole procedure. Investigations are also be performed on this matter.

BYPASS TRANSITION

The scenario investigated is Bypass Transition in zero-pressure-gradient boundary layers. It has been shown both experimentally as well as theoretically that the asymptotic solutions given by the classical stability analysis are inadequate to predict transition in wall-bounded shear flows. In some cases growth of energy can be observed even if the flow is stable. This can be explained by the fact that the operator describing the flow dynamics is non-normal. This type of transition scenario is observed when the boundary layer is subject to free turbulence of levels higher than 0.5–1%. In this case the classical TS-waves scenario is bypassed.

The most dangerous perturbations are streamwise counter rotating vortices. The vortices lift slow moving fluid from the area near the wall and pull fast moving fluid from the free stream above leading to the creation of alternating regions of fast and slow moving fluid, called *streaks*. The streaks grow as they travel downstream, start to oscillate and induce regions of chaotic swirly motion. These areas are called *turbulent spots*. The leading edge of the spots travel more or less at the free stream velocity U_∞ while the trailing edge at half of it. Thus the spots become more and more elongated and eventually start to merge with each other. After that fully turbulent flow develops and the transition is concluded. This flow reproduces the main features of a turbulent flow so it can be used as a model for the control of turbulent flows.

FEEDBACK CONTROL

Linear stability analysis can help understanding the transitional mechanisms is shear flows. However, it can also be used as a tool to actively reduce the perturbation strength and prevent transition. The procedure adopted here is *feedback control based on noisy measurements* (Chevalier et al. 2006). Data from the flow are used to calculate the control signal to be applied back to the flow.

The controller is acting on the flow through blowing and suction at the wall. The control requires knowledge of the full velocity field so the estimator is used to reconstruct the flow field from measurements taken on a stripe at the wall. Control can be applied both in the real and in the estimated flow. The combination of the estimation and the full information control is called *compensator*.

Control

Here follows the description of the full information controller. It is assumed that the exact state of the system is known. The linearised form of the Navier-Stokes in wall-normal velocity and wall-normal vorticity formulation

$$\frac{\partial}{\partial t}\begin{pmatrix} \hat{v} \\ \hat{\eta} \end{pmatrix} = \begin{pmatrix} \mathcal{L}_{OS} & 0 \\ \mathcal{L}_C & \mathcal{L}_{SQ} \end{pmatrix}\begin{pmatrix} \hat{v} \\ \hat{\eta} \end{pmatrix} \tag{1}$$

will be the model for the flow. Control emerges through non homogeneous boundary conditions.

To adopt the same formulation as in classical control theory, the control signal is expressed in the equations as a volume forcing by the lifting procedure. To account for measurement errors and non-modelled dynamics, such as non-parallel effect and nonlinearities, external excitation is added so that two extra forcing terms appear in the equations

$$\frac{\partial q}{\partial t} = \mathcal{A}q + B_1 w + B_2 u \tag{2}$$

where $B_1 w$ is the forcing due to external excitations of stochastic nature w and $B_2 u$ is the forcing from the control signal u. In feedback control the signal is calculated from the state q itself so $B_2 u = B_2 K q$ where K is the control gain.

The aim of the control is to minimise the kinetic energy of the perturbation while limiting the control effort. Thus the controller is designed so that the following objective function is minimised

$$\mathcal{F} = E(\|q\|^2 + l^2\|u\|^2) \tag{3}$$

The norm $\|q\|^2$ here is the kinetic energy of the perturbations, $\|u\|^2$ is the control effort and l is the actuation penalty.

In the discrete case the solution to this optimisation problem is given by the *Riccati equation*

$$A^*X + XA - \frac{1}{\epsilon}XBB^*X + Q = 0 \tag{4}$$

with the control gain computed by

$$K = -\frac{1}{l^2}B^*X \tag{5}$$

The Riccati equation is solved for each streamwise and spanwise wavenumber pair (k_x, k_z) separately.

Estimation

The state estimation problem is mathematically similar to the feedback control problem even though it is far away conceptually. Measurements are taken from the wall and the *sensors* responsible for the measurements include *noise*. The estimator can be seen as a filter-operator which has as input the measurements from the real flow and output the estimated flow. It is often called *Kalman filter*.

In the numerical estimation problem there are two flow fields. The 'real' flow and the estimated flow. In general all the quantities that correspond to the estimated flow will be marked with a hat $(\hat{\cdot})$.

The system to be solved is

$$\frac{\partial \hat{q}}{\partial t} = \mathcal{L}\hat{q} - f \tag{6}$$

where f is the feedback forcing term that will be a function of the difference between the real and the estimated flow. It is defined as

$$f = L(r - \hat{r}) \tag{7}$$

where r indicates the measurements. L is the feedback operator. The measurements are extracted from each state through the measurement operator

$$r = Cq \quad \text{and} \quad \hat{r} = C\hat{q} \tag{8}$$

The aim of the estimation problem is to minimise this error so the objective function here is

$$\mathcal{F} = E\|\tilde{q}\|^2 \tag{9}$$

From the equations above the mathematical similarity between the feedback control and the estimation problem is evident. We are looking for the optimal L for which the objective function is $\mathcal{F}$ is minimised. The optimisation problem

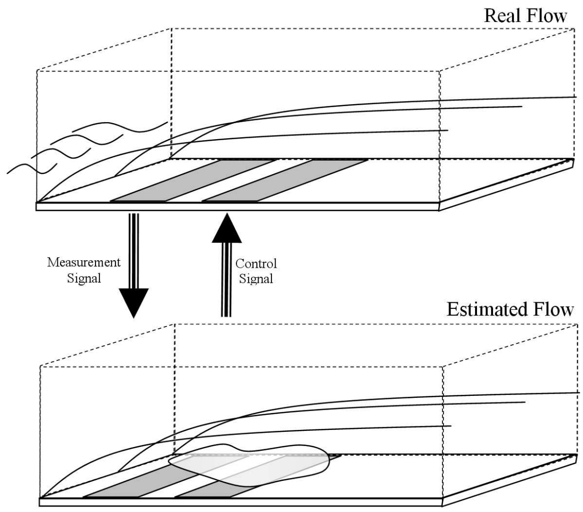

Figure 1: A schematic drawing of the compensator. The real flow is sending the measurements to the estimator while it sends back the control signal.

again is solved numerically through a Riccati equation similar to the one in the feedback control problem.

$$A\hat{P} + \hat{P}A^* - \hat{P}C^*G^{-1}C\hat{P} + M = 0 \tag{10}$$

where M is the covariance matrix of $B_1 w$ and G is the covariance matrix of the sensor noise. The estimation feedback gain is $L = -\hat{P}C^*G^{-1}$.

Three quantities are measured on the wall, the streamwise and spanwise skin friction and the pressure.

The Kalman filter presented here is linear estimation and it is the optimal case for a linear setting. The above theory though will be applied in a highly non linear case. Thus the performance of the estimation will be lower than the 'optimal'. One alternative to that is to use the full (non-linear) equations when solving the estimator while the gains used are computed with the linear theory. This is the *extended Kalman filter* and it is expected to be more accurate than the standard Kalman filter.

Compensator

The *compensator* is a combination of the full information control and the state estimation. The measurements are taken from the real flow, sent to the estimator where they are used to compute the forcing used to reproduce the perturbations in the real flow. Then the control is turned on. The control signal is computed for the estimated flow and it is both applied to the estimated and the real flow. The overall system is presented below

$$\begin{pmatrix} \dot{q} \\ \dot{\hat{q}} \end{pmatrix} = \begin{pmatrix} A & B_2K \\ -LC & A + B_2K + LC \end{pmatrix} \begin{pmatrix} q \\ \hat{q} \end{pmatrix} + \begin{pmatrix} B_1 & 0 \\ 0 & -LC \end{pmatrix} \begin{pmatrix} w \\ g \end{pmatrix} \tag{11}$$

The compensator problem as it was stated here accounts only for parallel flows. Further, it assumes that measurements and blowing/suction are taken/applied continuously over the whole domain. This theory is applied to a spatial boundary layer and both measurements and actuation are taken/applied on a part of the domain. Two locations need to be specified, one for the control and one for the estimator, where the local velocity profiles are taken to be used in the Orr–Sommerfeld/Squire operator. The flow is assumed to be locally parallel around these locations in order to solve the control and estimation problems. Once the control and estimation gains are calculated, the actuation forcing is cut with two smooth step functions around the chosen locations.

NUMERICAL SIMULATIONS

The simulation code (Lundbladh et al. 1999) employed for the present computations uses spectral methods to solve the three-dimensional, time dependent, incompressible Navier-Stokes equations. The algorithm uses Fourier representation in the streamwise and spanwise directions and Chebyshev polynomials in the wall-normal direction, together with a pseudo-spectral treatment of the nonlinear terms. The time advancement used is a four-step low-storage third-order Runge-Kutta method for the nonlinear terms and a second order Crank-Nicolson method for the linear terms. To correctly account for the downstream boundary layer growth a spatial technique is necessary. This requirement is combined with the periodic boundary condition in the streamwise direction by the implementation of a 'fringe'. In this region, at the downstream end of the computational box, a forcing is smoothly raised from zero, which causes the out-flowing disturbances to be damped and the flow is forced to the desired inflow condition.

Free–stream turbulence generation

The boundary layer considered here is subject to external disturbances, in particular *free–stream turbulence*. A superposition of eigenmodes of the Orr-Sommerfeld/Squire operator from the continuous spectrum is used to represent the inflow disturbance (Brandt et al. 2004). The disturbances are introduced in the fringe region.

Large–eddy simulations

Since for LES the size of the scales that must be resolved on the computational grid are much larger than in DNS, the resolution can be smaller and thus the computational cost is reduced significantly (typically of order 1%).

According to Schlatter et al. (2004) and Schlatter et al. (2006) the application of LES in transitional and turbulent flows has been found to work notably well as it has provided some very accurate results with much lower computational cost. In transitional flows there is considerable interaction between the base flow and the various instability modes and that can change the physical passing from laminar to turbulent flow.

When the Navier-Stokes equations are filtered a stress term appear which needs to be modelled. In our case this term will be modelled with the Relaxation Term model (ADM–RT). The relaxation term is incorporated to damp energy from the high frequency oscillations. According to Stolz et al. (2001) it acts only on the scales close to the numerical cut–off and is used to model the interaction between the resolved scales and those not represented in the numerical grid. The three–dimensional filter was used by Schlatter (2005) to evaluate the relaxation term. The complete system of LES equations for the RT model is obtained as

$$\frac{\partial \bar{u}_i}{\partial t} + \frac{\partial \bar{u}_i \bar{u}_j}{\partial x_j} = -\frac{\partial \bar{p}}{\partial x_i} + \frac{1}{Re}\frac{\partial^2 \bar{u}_i}{\partial x_j \partial x_j} - \mathcal{X} H_N * \bar{u}_i \qquad (12)$$

Table 1: Turbulence intensity (Tu), Resolution and box dimensions for the simulations. The box dimensions include the fringe region and are made dimensionless with respect to δ_0^*.

Method	Tu %	$x_l \times y_l \times z_l$ δ_0^*	$n_x \times n_y \times n_z$ $(resolution)$
DNS	4.7	$1000 \times 60 \times 50$	$1024 \times 121 \times 72$
LES	4.7	$1000 \times 60 \times 50$	$256 \times 121 \times 36$
LES	4.0	$2000 \times 60 \times 180$	$512 \times 121 \times 128$
LES	3.0	$2000 \times 60 \times 50$	$512 \times 121 \times 36$

Table 2: Control penalties, blowing and suction strip and location of the base flow target profile.

Control penalties	l	10^2
	r^2	0
$Re_{x_{start}}$		5.3×10^4
$Re_{x_{end}}$		1.4×10^5
target profile location		9×10^4

H_N here is the corresponding high pass filter.

RESULTS

Based on the theory and numerics presented in the previous sections, simulations of feedback control in a flat-plate boundary layer subject to free stream turbulence are performed. The parameters of the configuration are chosen so that the flow is transitional. The simulations presented here were performed with LES, while DNS results from earlier studies were used to validate the LES.

The parameters defining the problem are the Reynolds number, the intensity of the free-stream turbulence and the size of the computational box. The Reynolds number can be defined by means of the free stream velocity and the boundary layer displacement thickness δ^* or the distance from the leading edge x. The inflow Reynolds number is defined by the displacement thickness of the boundary layer at the inflow boundary of the computational domain Re_{δ^*} was chosen 300. All the quantities are made non dimensional with the displacement thickness δ^*, and the free-stream velocity.

For the case of $Tu = 4.7\%$ the length of the computational box needed to capture all the transition process is 1000, whereas at $Tu = 3.0\%$ and $Tu = 4.0\%$ it is 2000.

LES & DNS comparison

Since LES is used, the first step is to validate the method by comparing some LES results with DNS. The DNS simulation was performed by Brandt and Henningson (2004). The simulations are relative to full information control with $Tu = 4.7\%$. The parameters of the control, the control penalties, the region of blowing and suction and the base flow target profile are shown in table 2.

In figure 2 the wall-normal maximum of the streamwise velocity perturbation is shown for the uncontrolled case, DNS of full information control and LES of the same configuration. The results are obtained by averaging in time and in the spanwise direction. This quantity is selected since it indicates the growth of the streaks inside the boundary

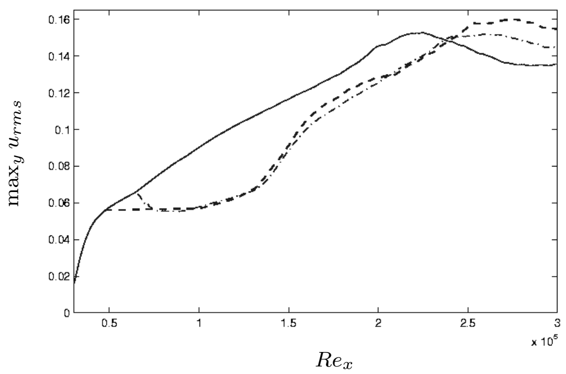

Figure 2: Wall normal maximum u_{rms}. *nocontrol*; — ,*DNS*; -·- ,*LES*; - - -.

Table 3: Study cases v.s control region. The initial and final location of control region are given in Re_x.

	Start (Re_x)	Finish (Re_x)
Case1 (no control)	—	—
Case2	5.3×10^4	1.4×10^5
Case3	5.3×10^4	1.9×10^5
Case4	5.3×10^4	2.3×10^5

layer. It can be seen that using LES-(ADM-RT) gives very similar results to the DNS simulations. In both cases control is reducing the streak growth equally. The rest of the results presented here are thus produced with LES.

Full information control

The first step of applying control theory to a boundary layer subject to free–stream turbulence is to design a reasonably good full information controller. This can be used as reference for the compensation, since the best possible performance is expected when the whole flow field is exactly known. The simulated flow for this case was subject to free-stream turbulence of intensity $Tu = 4.7\%$. A study on the effect of the control strip length on the quality of the control is performed. Case1 is the reference case where no control is applied, whereas in Case2, Case3 and Case4 blowing and suction is applied at the wall through a strip of different length. The values used are reported in table 3.

In figure 3-(a) the wall-normal maximum of the streamwise velocity perturbation is shown. As it can be seen from this figure the control is able to reduce the streak growth as long as it is active and this implies a delay of the transition location. It can also be seen that the longer the control region the later the transition occurs. However downstream of the control region, the u_{rms} grows rapidly to the same amplitude for all control lengths. In figure 3-(b) the friction coefficient is displayed for the three cases; also the values for a laminar and turbulent boundary layer are reported for comparison. It can be seen that for Case2 the friction coefficient is rising after the control region to values similar to the uncontrolled case (Case1), while in Case3 and Case4 it remains lower at the end of the computational domain.

The perturbation kinetic energy production is considered to characterise the effect of the blowing/suction at the wall. It is noted that negative production is achieved for a very short distance at the beginning of the control interval. The

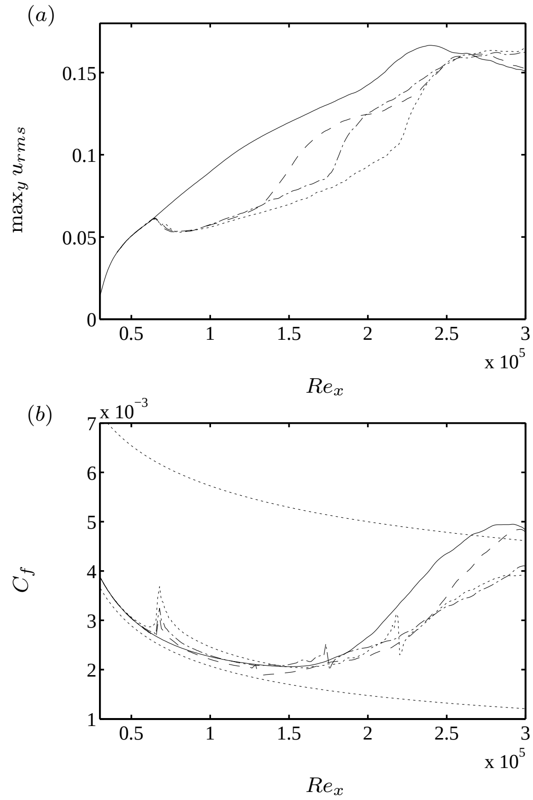

Figure 3: (a)Wall normal maximum u_{rms}, (b) friction coefficient. *Case*1; — ,*Case*2; - - - ,*Case*3; -·- ,*Case*4; · · ·

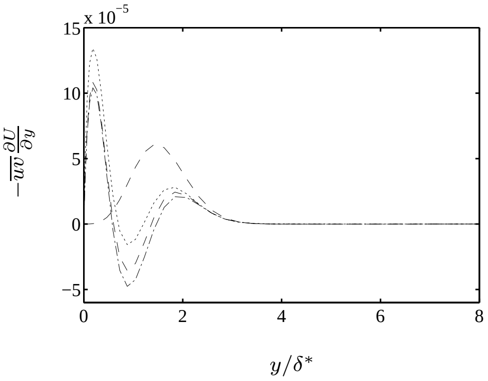

Figure 4: Wall normal profiles of Turbulent production at $Re_x = 3.6 \times 10^4$. *Case*1; — ,*Case*2; - - - ,*Case*3; -·- ,*Case*4; · · ·

production is plotted for $Re_x = 3.6 \times 10^4$ in figure 4. The decrease of production in the middle of the boundary layer is accompanied by an increase closer to the wall, where blowing and suction are active. As a consequence, the streamwise component of the perturbation velocity, the most relevant component, is characterised by a double-peak profile. The decrease of the turbulent production is due to a decrease of the Reynolds stress $-\overline{uv}$, being the mean velocity U only slightly changed by the control. The wall normal profiles of u_{rms} can be seen in figure 5.

State estimation

When tuning the estimator the parameters that define the strength of the forcing that is applied to the system, the sensor noise parameters, needs to be determined. The optimal set of values were chosen after performing several tests.

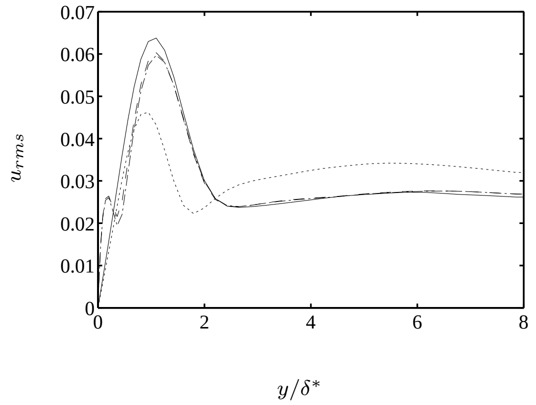

Figure 5: Wall normal profiles of u_{rms} at $Re_x = 3.6 \times 10^4$. $Case1$; — ,$Case2$; - - - ,$Case3$; -·- ,$Case4$; $\cdots$

Note that a relatively large value of the pressure sensor is needed to achieve good estimation. This actually limits the use of this measurement and can be explained by the fact that the pressure at the wall appear to be more sensitive to the free-stream turbulence than to the streaks inside the boundary layer. Further, at these high levels of perturbation, estimation is found to work better if the forcing is active only on the largest relevant scales. The estimation problem is applied to the case of $Tu = 3.0\%$ and $Tu = 4.0\%$.

Two different criteria were used to determine the performance of the estimator. The first was by looking at the instantaneous velocity field: One example of this comparison can be seen in figure 6. The second, more systematic way, was by calculating the estimation error given by

$$\epsilon = \frac{\int_{\Xi}(q-\hat{q})d\Xi}{\int_{\Xi}(q)d\Xi} \tag{13}$$

where Ξ is the region selected to evaluate the estimation error. In this case the region used is a plane parallel to the wall at height $y = 2$, comprising the whole measurement strip.

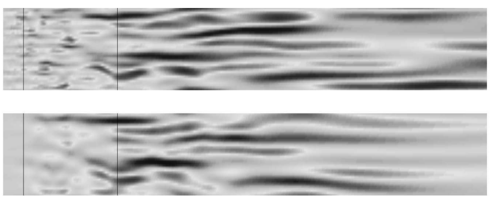

Figure 6: Instantaneous streamwise velocity fields. The upper is the real flow and the lower the estimated flow. The measurement strip is indicated with two vertical lines.

In figure 7 the wall-normal maximum of the streamwise velocity perturbation is shown for both the real and the estimated flow for the two different turbulence intensities. For the real flow one can see the streaks forming and growing. However, for the case of $Tu = 3.0\%$ the box is not long enough for transition to turbulence to occur. It can be seen that in the estimated flow the streaks decay downstream of the measurement region.

In figure 8 the wall normal profiles of u_{rms} are shown. It can be seen that the streaks are a bit weaker in the estimated flow than in the real flow. Perturbations in the free stream are not reproduced in the estimator. The estimation is more accurate closer to the wall.

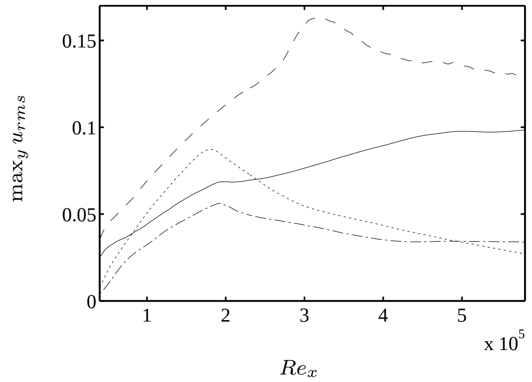

Figure 7: Wall normal maximum of u_{rms}. Real flow; (——) and Estimated flow; (–·–·–) for $Tu = 3.0\%$ and Real flow; (– – –) and Estimated flow; ($\cdots\cdots$) for $Tu = 4.0\%$.

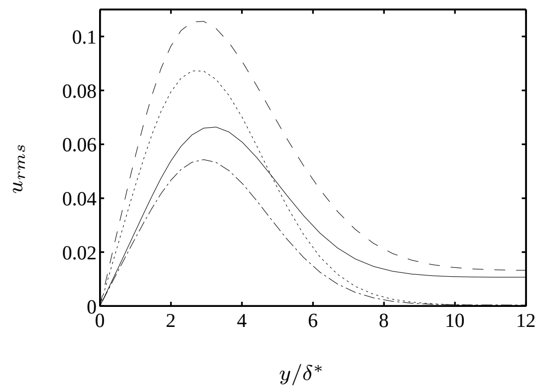

Figure 8: Wall normal profile of u_{rms} at $Re_x = 3.0 \times 10^5$. Real flow; (——) and Estimated flow; (–·–·–) for $Tu = 3.0\%$ and Real flow; (– – –) and Estimated flow; ($\cdots\cdots$) for $Tu = 4.0\%$.

Table 4: Cases studied.

Case	Description	Marker
Case1	Real flow with no control	– – –
Case2	Estimated flow with no control	–·–·–
Case3	Real flow with compensator	———
Case4	Estimated flow with full information control	$\cdots\cdots$
Case5	Real flow with full information control	–⋆–⋆–

Compensator

The final stage is combining the full information controller and the estimator into the compensator. The procedure requires first the estimator to run for a while without the control so that there is time for convergence. After this initial time the control is turned on. The estimation strip is the same as the one found as optimal in the previous paragraph while the control strip was chosen to start at $Re_x = 3.0 \times 10^5$ and finish at $Re_x = 5.4 \times 10^5$. In the following figures five different cases are presented. In table 4 it can be seen to which case each line in the plots corresponds to. The compensator is applied only for the 3.0% turbulence intensity.

In figure 9 the wall-normal maximum of the streamwise velocity perturbation is shown. The full information control effectively reduces the streaks amplitude while in the com-

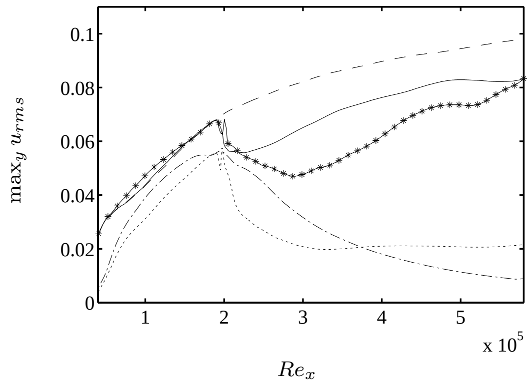

Figure 9: Wall normal maximum u_{rms}. *Case*1; – – – ,*Case*2; –·– ,*Case*3; ——, *Case*4; · · ·, *Case*5; –⋆–.

pensated flow, that reduction is not so effective. In principle in the estimated flow full information control is applied and it can be seen that the control works very satisfactorily as the streaks are completely damped and the flow is almost fully laminar.

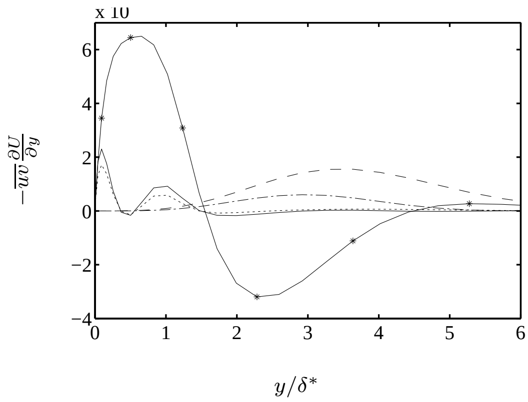

Figure 10: Wall normal profiles of Turbulent production at $Re_x = 3.3 \times 10^5$. *Case*1; – – – ,*Case*2; –·– ,*Case*3; ——, *Case*4; · · ·, *Case*5; –⋆–.

The perturbation kinetic energy production is considered to characterise the effect of the blowing/suction at the wall. The production is plotted within the control region at $Re_x = 3.3 \times 10^5$. From this plot it can be seen that the turbulence production increases near the wall while it decreases farther up in the boundary layer. In the compensator a slight reduction over the whole profile is observed. In the estimated flow the production is reduced almost to zero. The wall normal profiles of u_{rms} are depicted in figure 11.

CONCLUSIONS

Feedback control is applied to boundary-layer flows subject to high levels of free stream turbulence where the bypass transition occurs. In this specific application linear parallel theory is used to control a highly nonlinear spatial transitional flow. From the results presented, it can be seen that control is able to delay the growth of the streaks, which is responsible, through their secondary instabilities, for the considered bypass transition scenario. However the effectiveness of the measurment based estimator is limiting the performance of the control. Further, Brandt and Henningson (2004) observed that, if too strong localised blowing is applied, turbulent spots are induced by local instabilities

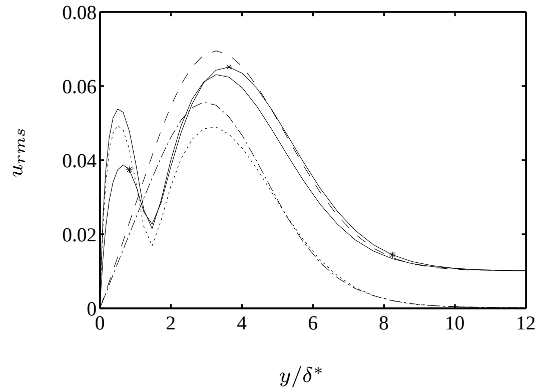

Figure 11: Wall normal profiles of u_{rms} at $Re_x = 3.3 \times 10^5$. *Case*1; – – – ,*Case*2; –·– ,*Case*3; ——, *Case*4; · · ·, *Case*5; –⋆–.

due to wall-normal inflectional profiles. An improvement of the transition delay can therefore be expected by limiting the blowing at the wall. The results further show that large-eddy simulations can be used as an efficient tool for both model reduction and studing the performance of a control strategy.

The present work is supported by the EOARD grant FA8655-04-1-3032 which is gratefully acknowledged.

REFERENCES

Bewley, T. R. 2001 "Flow control: New challenges for a new Renaissance". *Prog. Aerosp. Sci.* Vol. 37, pp. 21.

Brandt, L. and Henningson, D. S., 2004 "Linear feedback control of perturbations developing in a boundary layer under free-stream turbulence." In Advances in Turbulence X, Proc. of the Tenth European Turbulence Conference (eds. H. I. Andersson & P. A. Krogstad), pp. 767-770. CIMNE.

Brandt, L., Schlatter, P., and Henningson, D. S., 2004 "Transition in boundary layers subject to free-stream turbulence." *J. Fluid Mech.* Vol. 517, pp. 167-198.

Chevalier M., Hoepffner, J., Åkervik E., and Henningson, D. S., 2007 "Linear feedback control and estimation applied to instabilities in spatially developing boundary layers." *J. Fluid Mech.*, to appear.

Högberg, M., and Henningson, D. S., 2002 "Linear optimal control applied to instabilities in spatially developing boundary layers." *J. Fluid Mech.* Vol. 470, pp. 151.

Kim, J. 2003 "Control of turbulent boundary layers". *Phys. Fluids.* Vol. 15 (5), pp. 1093.

Lundbladh, A., Berlin, S., Skote, M., Hildings, C., Choi, J., Kim, J. and Henningson, D. S., 1999 "An efficient spectral method for simulation of incompressible flow over a flat plate." Technical Report KTH/MEK/TR-99/11-SE. KTH, Department of Mechanics, Stockholm.

Schlatter, P., 2005 "Large-eddy simulations of transition and turbulence in wall-bounded shear flows." PhD thesis, ETH Zurich, Switzerland.

Schlatter, P., Stolz, S. and Kleiser, L., 2004 "LES of transitional flows using the approximate deconvolution model." *Int. J. Heat Fluid Flow* Vol. 25 (3), pp. 549-558.

Schlatter P., Stolz, S. and Kleiser L., 2006 "LES of spatial transition in plane channel flow." *J. Turbulence* Vol. 7 (33), pp. 1-24.

Stolz, S., Adams, N. A. and Kleiser, L., 2001 "An approximate deconvolution model for large-eddy simulation with application to incompressible wall-bounded flows." *Phys. Fluids* Vol. 13 (4), pp. 997-1015.